

Empathy Modeling in Active Inference Agents for Perspective-Taking and Alignment

Mahault Albarracin

*Laboratoire d'ANalyse Cognitive de l'Information,
Universite du Quebec a Montreal, Quebec, Canada
Centre of Excellence for AI and Robotics,
Sheffield Hallam University, Sheffield, UK*

Anna Mikeda

Glass Umbrella, USA

Alejandro Jimenez Rodriguez*

*Centre of Excellence for AI and Robotics,
School of Computing and Digital Technologies
Sheffield Hallam University, Sheffield, UK*

Sanjeev V Namjoshi[†] and Philip Wilson[‡]

Independent researcher

Dalton A R Sakthivadivel[§]

Department of Mathematics, CUNY Graduate Centre, New York, NY 10016

Hongju Pae[¶]

Active Inference Institute, California, USA

Harshil Shah

Mission San Jose High School, Fremont, California, USA

(Dated: February 25, 2026)

Artificial agents capable of understanding and aligning with others' intentions are essential for safe and socially robust artificial intelligence. We introduce a computational framework for empathy in active inference agents, grounded in explicit perspective-taking via self-other model transformation. Rather than maintaining

separate generative models for each interaction partner, agents dynamically reconfigure a single generative model between egocentric and allocentric interpretations, enabling principled inference over others’ beliefs, goals, and action tendencies.

We instantiate this framework in a multi-agent Iterated Prisoner’s Dilemma and show that empathic perspective-taking induces robust cooperation without explicit communication or reward shaping. Cooperation emerges only when empathy is reciprocated, while asymmetric empathy leads to systematic exploitation. Beyond equilibrium outcomes, empathic agents exhibit synchronized behavior, rapid recovery from stochastic defections, and joint intentional dynamics resembling apology–forgiveness cycles. Near empathy symmetry, interactions display long transients and elevated variance, consistent with critical dynamics near regime boundaries.

We further examine a learning-enabled variant in which agents infer opponent type via Bayesian updating. While opponent models converge rapidly, long-run cooperation remains primarily determined by the empathy parameter, indicating that cooperation is driven by empathic structure rather than learned reciprocity. Together, these results demonstrate that empathy functions as a structural prior over social interaction, shaping coordination stability, robustness, and temporal dynamics. The proposed framework highlights active inference as a principled foundation for socially aligned artificial agents that coordinate through internal simulation rather than behavioral mimicry.

I. INTRODUCTION

Artificial agents that can understand and share perspectives are crucial for achieving alignment with human values in complex social interactions Dautenhahn (1998). Traditional approaches to artificial empathy often rely on surface-level pattern recognition and scripted emotional responses, which lack the deeper phenomenological grounding of true human empathy Howcroft and Blake (2025). This results in an “empathy gap” where AI

* a.jimenez-rodriguez@shu.ac.uk

† sanjeev.namjoshi@gmail.com

‡ philipollaswilson@protonmail.com

§ dsakthivadivel@gc.cuny.edu

¶ hjpae@activeinference.institute

responses, although appropriate in form, do not reflect genuine understanding. To bridge this gap, we propose an active inference framework in which agents treat others’ preferences and social valuation as latent variables to be inferred. Our agents internally model and update beliefs about others’ mental states, including their degree of prosocial concern, and incorporate these beliefs into action selection through an explicit tradeoff between pragmatic and epistemic value, enabling socially aligned behaviour grounded in principled uncertainty reduction. It is worth distinguishing the components of empathy this framework engages. Cognitive science identifies at least three dissociable facets: cognitive empathy (inferring another’s mental states, closely related to theory of mind), affective empathy (resonating with another’s emotional states), and a motivational component, empathic concern and the desire to promote another’s well-being Weisz and Cikara (2021), Decety and Jackson (2004), Lamm et al. (2007). These components are neurally and functionally dissociable Shamay-Tsoory et al. (2009), Arioli et al. (2021). Prior computational work on theory of mind in active inference has engaged primarily the cognitive dimension, predicting what another agent will do. Our framework goes further. We introduce an empathy parameter λ which governs how much weight an agent places on the other’s expected free energy during planning. λ makes the other’s welfare salient within the agent’s own decision-making, operationalizing empathic concern within the variational framework, akin to some game theoretic approaches Orbell and Dawes (1993), Rabin (1993), Hwang et al. (2018). In this sense, our model engages the affective dimension (through valenced evaluation of the other’s outcomes) and provides a structural placeholder for the motivational dimension, though in the present implementation the degree of empathic concern is set exogenously rather than arising from the agent’s own need dynamics. Our approach draws inspiration from human cognition and neuroscience. In humans, the mirror neuron system supports simulation of others. Observing another’s action activates one’s own motor and emotional representations Oberman and Ramachandran (2007). Similarly, our agent models others using a generative architecture structurally matched to its own, while treating agent-specific parameters as latent variables to be inferred online. Rather than hard-coding opponent characteristics, the agent maintains a posterior distribution over behavioral and empathic parameters, effectively reusing its own cognitive machinery to “step into their shoes” while updating its beliefs through experience. This design aligns with simulation-theoretic accounts of social cognition Goldman (2006) and with theories of second-person neuroscience that emphasize modeling others

within one’s own cognitive framework Redcay and Schilbach (2019), Lehmann et al. (2024). Prior work has begun integrating theory-of-mind (ToM) into active inference. For example, Demekas et al. (2023) model two agents in an Iterated Prisoner’s Dilemma (IPD) as a coupled active inference system, revealing how learning rates and reward structures affect the emergence of cooperative or defection strategies. More recently, Pitliya et al. (2025), Çatal et al. (2024) demonstrated that active inference agents with explicit ToM achieve improved cooperation without requiring explicit communication, though in some cases through belief sharing. Matsumura et al. Matsumura et al. (2024) introduce an empathic extension of active inference in which an agent reuses a structurally matched generative model to simulate another agent’s perspective, consistent with simulation-theoretic accounts of social cognition. In their formulation, the agent incorporates estimates of the other’s internal state into policy evaluation and can select actions that reduce the other agent’s expected free energy, promoting socially appropriate behavior in embodied navigation tasks. Their implementation is grounded in domain-specific dynamics (e.g., social-force models for multi-robot navigation) and focuses on improving coordination and safety margins in situated environments. While this work demonstrates that active inference can support empathic behavior in embodied settings, it does not examine repeated strategic interaction under simultaneous decision-making, nor does it analyze equilibrium structure, exploitation asymmetry, or regime-boundary dynamics. In contrast, our framework embeds empathic valuation within a formally specified game-theoretic setting, introduces latent inference over opponent valuation parameters, and characterizes how empathy reshapes stability, threshold behavior, and strategic foresight in iterated dilemmas. More broadly, prior active inference approaches to social interaction typically instantiate separate self- and other-models but do not treat opponent valuation itself as a hidden variable subject to epistemic inference, nor do they analyze how such latent social parameters alter equilibrium selection and dynamical stability. Moreover, these approaches remain within the cognitive empathy domain, they model what another agent will do, but not what it will experience or whether its welfare matters to the modeling agent. Our contribution is a unified algorithmic framework for empathy in active inference in which each agent maintains a generative model structurally matched to its own architecture when modeling others. Rather than hand-coding discrete opponent types, agent i represents agent j ’s behavioral and valuational parameters as latent variables and performs Bayesian inference over them online. This preserves a shared generative struc-

ture, common state space, transition dynamics, and observation mappings, while allowing agent-specific parameters governing cooperation bias, reciprocity, precision, and empathic valuation to be inferred from interaction history. Perspective-taking is realized as a continuous empathy-weighted blend of self- and other-oriented expected free energy:

$$\mathbf{G}_{\text{social}} = (1 - \lambda) \mathbf{G}_{\text{self}} + \lambda \mathbb{E}[\mathbf{G}_{\text{other}}], \quad (1)$$

where $\lambda \in [0, 1]$ controls the degree of empathic concern. The opponent’s empathic weighting is itself treated as a hidden variable, giving rise to epistemic value and principled exploratory behavior early in interaction. We formally integrate this mechanism into the active inference perception-action loop under simultaneous decision-making. The resulting agent plans using both pragmatic and epistemic components of expected free energy, leading to emergent pro-social behavior such as sustained mutual cooperation in strategic dilemmas where purely self-interested agents would defect.

II. METHODOLOGY

A. Generative Model for an Empathic Agent

We formalize each agent’s belief system as a *partially observable Markov decision process* (POMDP) generative model, extended to support perspective-taking (as demonstrated in Pitliya et al. (2025)). The agent maintains a probability distribution over latent hidden states, sensory observations, and actions/policies over time. Let s_τ denote the hidden state at time τ , o_τ the observation at time τ , and π a policy (a sequence of future control states u_τ). Under standard Markovian assumptions, the joint generative model factorizes as

$$P(\tilde{o}, \tilde{s}, \pi) = P(s_0) P(\pi) \prod_{\tau=1}^T P(s_\tau | s_{\tau-1}, u_\tau) \prod_{\tau=0}^T P(o_\tau | s_\tau), \quad (2)$$

where $\tilde{s} = (s_0, \dots, s_T)$ and $\tilde{o} = (o_0, \dots, o_T)$ denote state and observation trajectories, respectively.

Model parameters include the state-transition and observation likelihood mappings, commonly represented in active inference by tensors (or matrices) B and A , respectively, along with preferences over outcomes (prior over observations) C and initial state priors D . All random variables are discrete in our implementation. We further distinguish *first-order*

parameters (e.g., the entries of A, B, C, D) from *second-order* parameters that modulate learning rates and/or precision (inverse temperature) of the corresponding distributions.

Posterior inference is performed via variational Bayes. The agent maintains a recognition density $Q(s_\tau)$ that approximates the true posterior and updates this density by minimizing *variational free energy* (VFE). Intuitively, this corresponds to continually updating beliefs $Q(s_\tau)$ so as to better explain incoming observations under the agent’s generative model.

B. Hidden state factorization and observation modalities

In our model, each agent maintains a generative model over joint interaction outcomes. The hidden state s_τ is a single multinomial latent variable encoding the joint outcome of the current round:

$$s_\tau \in \{\text{CC}, \text{CD}, \text{DC}, \text{DD}\}, \quad (3)$$

where C and D denote cooperation and defection, and the pair indicates (my action, opponent’s action). This state space jointly encodes both the agent’s own behaviour and the opponent’s, providing the minimal sufficient representation for computing payoffs and planning future actions in a simultaneous-move game. The observation model is an identity mapping $A = I_4$, such that the agent directly observes the joint outcome at each round. This means the agent has full access to both its own and the opponent’s realised actions, but must infer the opponent’s *future* behaviour through Theory of Mind (Section ??).

Rather than introducing a binary latent variable to switch between egocentric and allocentric perspectives, our model implements perspective-taking as a *continuous blend* of self- and other-oriented expected free energy. For each candidate action a_i , the agent computes a social EFE:

$$\begin{aligned} \mathbf{G}_{\text{social}}(a_i) = & (1 - \lambda) \mathbf{G}_{\text{self}}(a_i \mid q(a_j \mid h_t)) \\ & + \lambda \mathbb{E}_{q(a_j \mid h_t)}[\mathbf{G}_{\text{other}}(a_j)], \end{aligned} \quad (4)$$

where $\lambda \in [0, 1]$ is the empathy parameter and $q(a_j \mid h_t)$ denotes the predicted opponent response conditioned on interaction history h_t . The empathy parameter λ is a fixed architectural parameter that determines the degree to which the agent weighs the other’s welfare in its own planning. At $\lambda = 0$, the agent is purely self-interested; at $\lambda = 1$, it is purely altruistic; intermediate values produce a graded trade-off between egocentric and allocentric evaluation.

The opponent’s predicted response $q(a_j | h_t)$ is obtained from a depth-1 Theory of Mind module that models the opponent as a rational agent whose behavioral and valuational parameters are treated as latent variables. In the static case, the prediction takes the form

$$q(a_j | h_t) \propto \exp(-\beta_j \mathbf{G}_j(a_j | h_t)), \quad (5)$$

where β_j is the opponent’s precision and $\mathbf{G}_j(a_j | h_t)$ is the opponent’s expected free energy computed using the inferred distribution over opponent parameters. When opponent inversion is active, this prediction is refined through Bayesian updating over latent behavioral parameters, and contributes both pragmatic and epistemic terms to policy evaluation (see Section III F). Because the opponent’s empathic weighting is treated as a hidden variable, action selection incorporates not only pragmatic value but also epistemic value, favoring actions that are informative about the opponent’s underlying social disposition.

The transition model B is parameterized as a set of action-conditional matrices $B^{(a_i)} \in \mathbb{R}^{4 \times 4}$, one for each of the agent’s two actions (cooperate or defect). Because the joint outcome also depends on the opponent’s action, which is not under the agent’s control, the transition matrices encode stochastic mappings that reflect uncertainty over the opponent’s response, distributing probability mass across the two possible outcomes consistent with each of the agent’s actions.

Each agent’s preferences are encoded in the vector $C \in \mathbb{R}^4$, which assigns a log-preference (or negative surprise) to each joint outcome. The preference vectors are set according to the standard Prisoner’s Dilemma payoff matrix (R=3, T=5, S=0, P=1), but from the agent’s own perspective. This ensures that the agent’s pragmatic EFE reflects the standard incentive structure of the game without any built-in bias toward cooperation.

C. Perspective-taking via structurally matched generative models

Central to our approach is the assumption that an agent models others using a generative architecture structurally matched to its own Ford et al. (2012). Let $M_{\text{self}}^i = (A_i, B_i, C_i, D_i)$ denote agent i ’s generative model of itself. When modeling agent j , the agent does not construct an arbitrary independent model; rather, it instantiates a generative model with identical structural form (state space, observation model, and inference machinery), while treating opponent-specific behavioral and valuational parameters as latent variables to be

inferred online.

Formally, we denote the opponent model as

$$M_{\text{other}}^i = (A, B, \theta_j), \quad (6)$$

where θ_j comprises latent parameters governing cooperation bias, reciprocity, precision, and empathic weighting. These parameters are updated via Bayesian inference over interaction history.

The resulting other-model shares the same structural form as the self-model—the same state and observation dimensions and the same PyMDP inference machinery—but differs in its parameterization, which is inferred rather than directly observed. This construction is inspired by simulation theory, according to which an agent understands others by reusing its own cognitive architecture under alternative parameter settings (Goldman 2006, Gallese and Goldman 1998).

In our implementation, the self-model and other-model are instantiated as separate but structurally matched generative models at the beginning of an interaction. The self-model M_{self}^i is used for state inference, while the other-model M_{other}^i is passed to a Theory of Mind module that predicts the opponent’s likely response based on interaction history (Section ??).

Perspective-taking does not occur via a latent mode-switching variable; instead, egocentric and allocentric evaluations are computed simultaneously and blended through the social expected free energy (social EFE):

$$\mathbf{G}_{\text{social}}(a_i) = (1 - \lambda) \mathbf{G}_{\text{self}}(a_i) + \lambda \mathbb{E}_{q(a_j | h_t)}[\mathbf{G}_{\text{other}}(a_j)], \quad (7)$$

where $\lambda \in [0, 1]$ is the empathy parameter and $q(a_j | h_t)$ denotes the predicted opponent response conditioned on interaction history h_t .

The opponent prediction is computed as a depth-1 best-response distribution under the inferred opponent parameters:

$$q(a_j | h_t) \propto \exp(-\beta_j \mathbf{G}_j(a_j | h_t)), \quad (8)$$

where \mathbf{G}_j is evaluated using the current posterior over θ_j . Because opponent valuation parameters are treated as hidden variables, action selection incorporates epistemic value, favoring actions that are informative about the opponent’s underlying social disposition.

This design has several important consequences. First, shared structural assumptions ensure that environmental dynamics and observation mappings remain aligned across perspectives. Second, the continuous empathy parameter λ provides a smooth interpolation between egocentric and allocentric evaluation. Third, the separation of *what the opponent will do* (Theory of Mind inference) from *how much to care* (empathic weighting) allows each component to be analyzed independently.

D. Active inference and sophisticated planning

Having specified the generative model for each agent, we now describe the inference and planning procedure that governs agent behaviour, inspired by sophisticated inference as described in Friston et al. (2021). Each agent operates in discrete perception–action cycles, alternating between variational state inference, opponent modelling, and policy evaluation. An overview is given in Algorithm 1. At each time step τ , the agent receives a joint-outcome observation $o_\tau \in \text{CC, CD, DC, DD}$ and updates its posterior beliefs $Q(s_\tau)$ over the four-state hidden variable by minimising variational free energy. This filtering step combines the predictive prior from the previous posterior and the transition model \mathbf{B} with the observation likelihood \mathbf{A} , using standard active inference state inference (Da Costa et al. 2020). In parallel with state inference, the agent maintains a parametric model of its opponent via a particle-based inversion module. Rather than enumerating discrete strategy types, each particle k carries a parameter vector

$$\theta_k = (\alpha_k, \rho_k, \beta_k, \lambda_{j,k}),$$

where α encodes cooperation bias, ρ reciprocity sensitivity, β behavioral precision, and λ_j the opponent’s empathic weighting.

The opponent’s probability of cooperation is modeled as

$$P(a_j = C \mid h_t, \theta_k) = \sigma(\beta_k(\alpha_k + \rho_k f(h_t) + \text{empathy_shift}(\lambda_{j,k}))), \quad (9)$$

where $f(h_t)$ is a history feature and σ the logistic function.

Particle weights are updated via Bayesian filtering:

$$w_k^{(\tau)} \propto w_k^{(\tau-1)} P(a_j^{(\tau)} \mid h_t, \theta_k). \quad (10)$$

The posterior-weighted ensemble yields the predictive distribution:

$$q_{\text{learned}}(a_j | h_t) = \sum_k w_k P(a_j | h_t, \theta_k). \quad (11)$$

Because the opponent’s empathic weighting λ_j is treated as a hidden variable, action selection incorporates epistemic value. For candidate action a_i , the epistemic component is defined as

$$G_{\text{epistemic}}(a_i) = -\mathbb{E} \left[\text{KL}(p(\theta_j | a_j^{(\tau+1)}, h_t) \| p(\theta_j | h_t)) \right], \quad (12)$$

which quantifies the expected information gain about the opponent’s latent parameters. Because the particle filter may be unreliable early in an interaction (when few observations have been collected), the agent gates between the learned posterior-predictive distribution and a static Theory of Mind (ToM) prior. In the static ToM, the opponent is modeled as selecting actions based only on interaction history h_t (rather than on the agent’s current-round action), consistent with simultaneous decision-making. The static ToM distribution is given by

$$q_{\text{static}}(a_j | h_t) \propto \exp(-\beta_j G_j(a_j | h_t)), \quad (13)$$

where β_j is the assumed opponent precision and $G_j(a_j | h_t)$ is the opponent’s expected free energy computed under the opponent’s inferred policy over the agent’s actions (estimated from history). Concretely, we form an empirical belief $\pi_i(a_i | h_t)$ over the agent’s own action (e.g., based on past cooperation rate), and evaluate

$$G_j(a_j | h_t) = - \sum_{a_i \in \{C, D\}} \pi_i(a_i | h_t) \text{payoff}_j(a_i, a_j). \quad (14)$$

The gated prediction smoothly interpolates between learned and static predictions based on the inversion reliability $r \in [0, 1]$, computed from the entropy of the particle weights:

$$q_{\text{gated}}(a_j | h_t) = r \cdot q_{\text{learned}}(a_j | h_t) + (1 - r) \cdot q_{\text{static}}(a_j | h_t). \quad (15)$$

When reliability is low (uniform weights, high entropy), the agent falls back to the static ToM prior; when reliability is high (weights concentrated), the learned model dominates.

Following state inference and opponent modelling, the agent evaluates candidate policies. We implement two planning regimes. In the *myopic* regime ($H = 1$), the agent evaluates a single-step total expected free energy for each candidate action $a_i \in \{C, D\}$ as

$$\begin{aligned} G_{\text{total}}(a_i) &= (1 - \lambda) G_{\text{self}}(a_i | q(a_j | h_t)) + \lambda \mathbb{E}_{q(a_j | h_t)} [G_{\text{other}}(a_j)] \\ &+ G_{\text{epistemic}}(a_i), \end{aligned} \quad (16)$$

where $G_{\text{self}}(a_i | q(a_j | h_t)) = -\mathbb{E}_{q(a_j|h_t)}[\text{payoff}_i(a_i, a_j)]$ is the agent’s expected negative payoff under the predicted opponent response, and $G_{\text{other}}(a_j)$ is the opponent’s expected negative payoff under the current posterior over opponent parameters. The epistemic term $G_{\text{epistemic}}(a_i)$ is the one-step-ahead expected information gain about the opponent’s latent parameters (including λ_j), operationalized as the expected KL divergence between the current posterior and the posterior after observing the opponent’s next action:

$$G_{\text{epistemic}}(a_i) = -\mathbb{E}_{a_j \sim q(\cdot|h_t, a_i)} [\text{KL}(p(\theta_j | h_{t+1}) || p(\theta_j | h_t))], \quad (17)$$

where θ_j denotes the opponent’s latent parameters (e.g., $(\alpha, \rho, \beta, \lambda_j)$) and h_{t+1} is the updated history after observing a_j .

In the *sophisticated* regime ($H > 1$), the agent enumerates all 2^H candidate policies $\pi = (a_i^{(0)}, a_i^{(1)}, \dots, a_i^{(H-1)})$ and evaluates each by forward rollout. At each rollout step t , the opponent’s response is predicted and the total expected free energy is accumulated:

$$G(\pi) = \frac{1}{H} \sum_{t=0}^{H-1} \left[(1 - \lambda) G_{\text{self}}^{(t)} + \lambda G_{\text{other}}^{(t)} + G_{\text{epistemic}}^{(t)} \right]. \quad (18)$$

At rollout step $t = 0$, the gated prediction $q_{\text{gated}}(a_j | h_t)$ is used; at future steps $t > 0$, the opponent prediction is conditioned on the simulated history induced by the partial rollout (i.e., past actions in the simulated future). The agent then forms a posterior over policies:

$$Q(\pi) \propto \exp(-\beta G(\pi)), \quad (19)$$

and marginalises to the first action:

$$P(a_i^{(0)} = a) = \sum_{\pi: \pi_0=a} Q(\pi). \quad (20)$$

An action is sampled from this distribution and executed. The perception–action cycle repeats at $\tau + 1$.

Algorithm 1 Active inference with empathic planning

- 1: Initialise beliefs $Q(s_0)$ with prior \mathbf{D} ; initialise particle filter with uniform weights over θ_j
 - 2: **for** $\tau = 0$ to T **do**
 - 3: Observe joint outcome o_τ
 - 4: Extract opponent action $a_j^{(\tau)}$ from o_τ
 - 5: Update particle weights: $w_k \leftarrow w_k \cdot P(a_j^{(\tau)} | h_t, \theta_k)$; normalise
 - 6: Update beliefs $Q(s_\tau)$ via variational state inference
 - 7: Compute reliability r from particle weight entropy
 - 8: Form predictions: $q_{\text{learned}}(a_j | h_t) = \sum_k w_k P(a_j | h_t, \theta_k)$
 - 9: Compute static ToM prior $q_{\text{static}}(a_j | h_t)$ via Eq. (13)
 - 10: Gate predictions: $q_{\text{gated}}(a_j | h_t) \leftarrow r q_{\text{learned}} + (1 - r) q_{\text{static}}$
 - 11: **for** each candidate policy $\pi = (a_i^{(0)}, \dots, a_i^{(H-1)})$ **do**
 - 12: **for** $t = 0$ to $H - 1$ **do**
 - 13: Predict opponent response $q(a_j | h_t^{(t)}) \leftarrow$ **if** $t = 0$: $q_{\text{gated}}(a_j | h_t)$; **else**: $q_{\text{static}}(a_j | h_t^{(t)})$
 - 14: Compute $G_{\text{self}}^{(t)}$ and $G_{\text{other}}^{(t)}$ under $q(a_j | h_t^{(t)})$
 - 15: Compute epistemic term $G_{\text{epistemic}}^{(t)}$ (one-step expected information gain)
 - 16: Accumulate $G^{(t)} \leftarrow (1 - \lambda)G_{\text{self}}^{(t)} + \lambda G_{\text{other}}^{(t)} + G_{\text{epistemic}}^{(t)}$
 - 17: **end for**
 - 18: $G(\pi) \leftarrow \frac{1}{H} \sum_t G^{(t)}$
 - 19: **end for**
 - 20: $Q(\pi) \propto \exp(-\beta G(\pi))$
 - 21: Marginalise: $P(a_i^{(0)} = a) = \sum_{\pi: \pi_0 = a} Q(\pi)$
 - 22: Sample and execute $a_i^{(\tau)} \sim P(a_i^{(0)})$
 - 23: **end for**
-

III. RESULTS

A. Iterated Prisoner’s Dilemma setup and global cooperation landscape

We first characterize the global cooperation landscape induced by empathic weighting in the Iterated Prisoner’s Dilemma (IPD). Across dyads, the empathy parameter λ functions as a control variable that reshapes equilibrium outcomes, inducing a sharp shift from mutual defection to sustained cooperation.

We evaluate the proposed model in the classic two-player IPD, a canonical paradigm for studying the emergence of cooperation under strategic tension Rapoport and Chammah (1965). In each round, both agents simultaneously select either cooperate (C) or defect (D). Payoffs follow the standard ordering $T > R > P > S$ (concretely $T = 5$, $R = 3$, $P = 1$, $S = 0$), where R is the mutual cooperation reward (C, C), T is the temptation payoff for unilateral defection (D, C), P is the mutual defection punishment (D, D), and S is the sucker’s payoff (C, D). This payoff structure captures the core dilemma that unilateral defection is individually advantageous ($T > R$), yet mutual cooperation yields higher collective welfare than mutual defection ($R > P$). Unless otherwise stated, simulations in this subsection use myopic planning ($H = 1$), no opponent-parameter inference (static ToM prediction only), and symmetric precision parameters. Each interaction consists of 100 repeated rounds.

Each agent is parameterized by an empathy level $\lambda \in [0, 1]$, which enters the social EFE as:

$$G_{\text{social}}(a_i) = (1 - \lambda) G_{\text{self}}(a_i \mid q(a_j \mid h_t)) + \lambda \mathbb{E}_{q(a_j \mid h_t)}[G_{\text{other}}(a_j)], \quad (21)$$

Here, setting $\lambda = 0$ yields a purely self-oriented agent, whereas $\lambda = 1$ yields a fully other-oriented agent. Intermediate values implement a graded tradeoff between self-interest and prosocial concern.

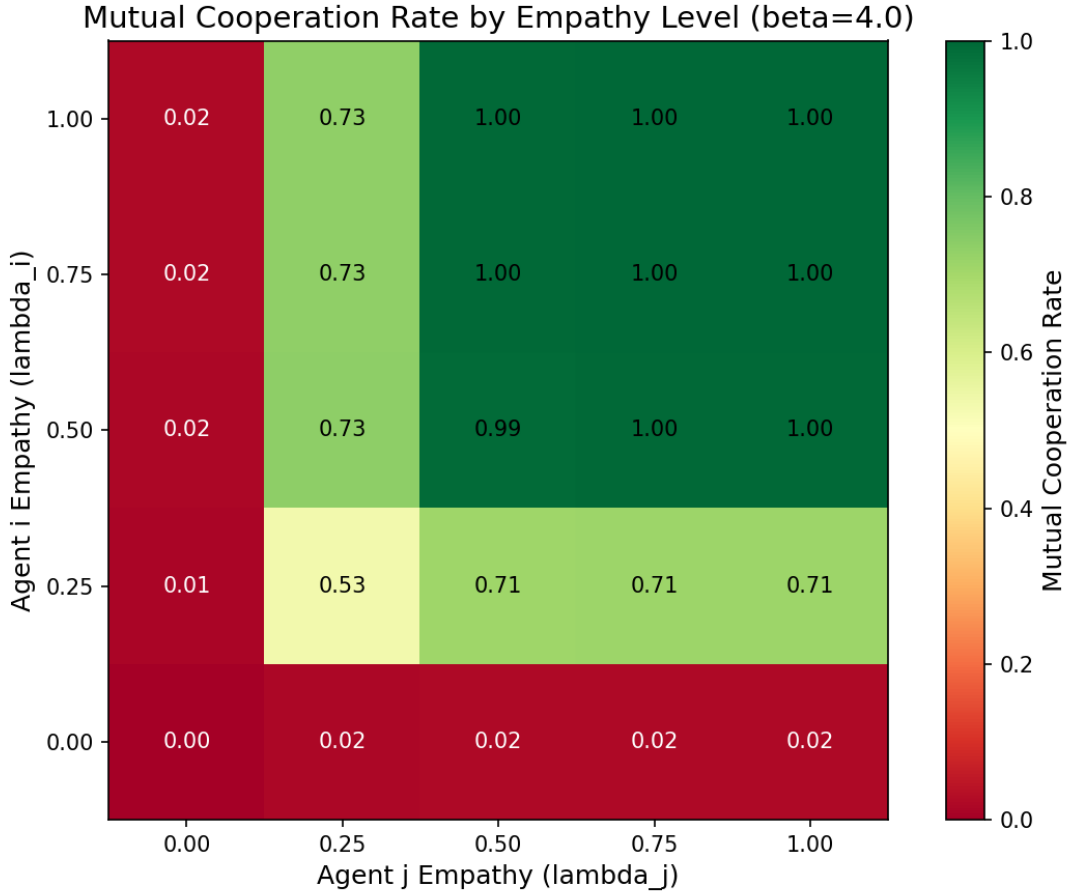


FIG. 1: Mutual cooperation landscape across dyadic empathy. Each cell shows the mean fraction of rounds ending in mutual cooperation (C, C), averaged over repeated simulations for the corresponding empathy pair (λ_i, λ_j) . Axes indicate the empathy parameters of the two agents λ_i and λ_j .

Figure 1 shows the fraction of rounds resulting in mutual cooperation (C, C) across the (λ_i, λ_j) grid. A clear regime structure emerges: for low empathy (bottom-left region), mutual cooperation rates remain near zero, and interactions converge to the mutual-defection equilibrium. As both agents' empathy increases beyond approximately $\lambda \gtrsim 0.25$ - 0.30 , however, the dyad rapidly shifts toward near-perfect cooperation, with mutual cooperation rates approaching unity.

Importantly, moderate increases in empathy around the threshold produce disproportionately large changes in cooperation frequency. The resulting landscape is consistent with a phase-like transition in which increasing empathic weighting λ shifts the dominant attractor

of the interaction from (D, D) to (C, C) .

Given these configurations, we next examine (1) the role of empathy symmetry and exploitation under asymmetric dyads, (2) temporal recovery dynamics and implicit communication, (3) boundary-layer variability near the cooperation threshold, and (4) an explicit characterization of the underlying transition point λ^* .

B. Emergent exploitation dynamics

While symmetric empathy supports stable cooperation, asymmetries in empathic weighting give rise to systematic *exploitation*. We therefore examine payoff outcomes under empathy imbalance.

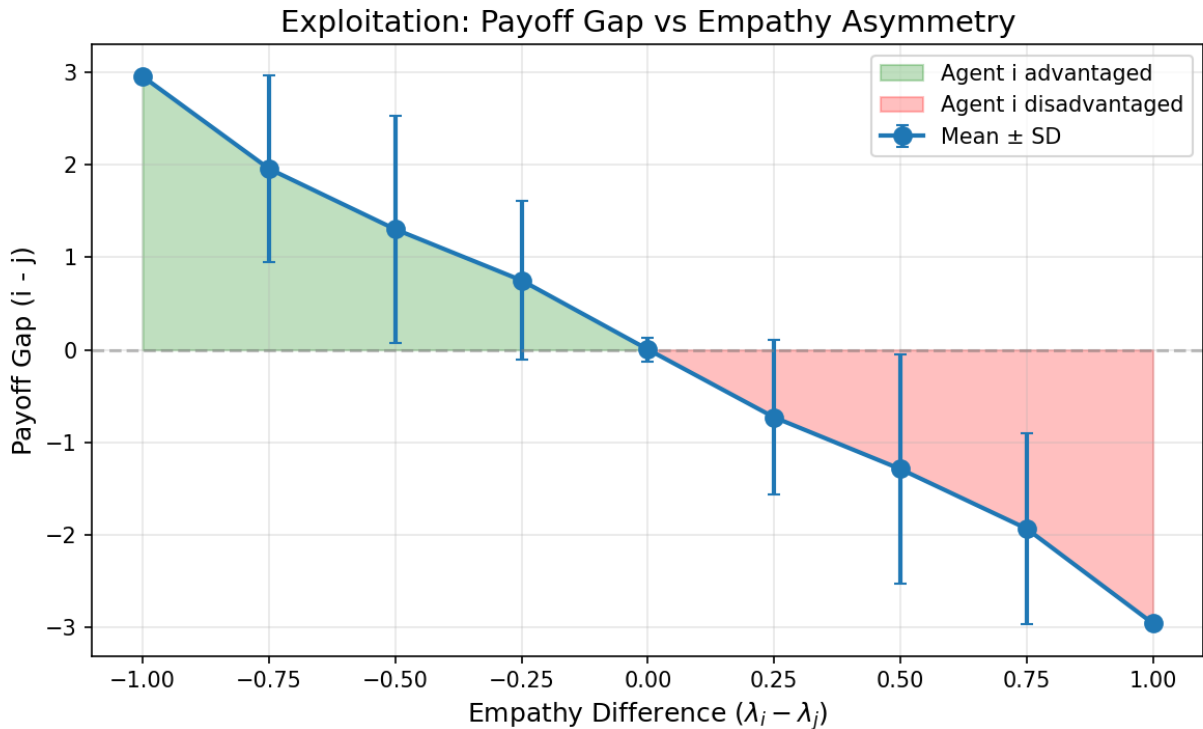


FIG. 2: Empathy asymmetry induces systematic exploitation. Mean payoff gap as a function of empathy difference $\lambda_i - \lambda_j$, where positive values indicate that agent i obtains higher average payoff. Error bars denote ± 1 standard deviation across runs aggregated within each rounded empathy-difference bin.

Figure 2 summarizes the resulting dynamics. The less empathic agent systematically

exploits the more empathic agent. When $\lambda_i \ll \lambda_j$, agent i assigns negligible weight to the other’s welfare and defects more frequently, while agent j , heavily weighting G_{other} , continues to cooperate despite being exploited. This produces a positive payoff gap in favor of the less empathic agent. The direction reverses when $\lambda_i \gg \lambda_j$, yielding symmetric exploitation in the opposite direction.

Importantly, the magnitude of the payoff gap increases approximately monotonically with empathy disparity over the tested range. This exploitation effect arises as a structural consequence of the social EFE formulation: increasing λ progressively reshapes the agent’s objective toward other-regarding valuation, thereby altering the stability of unilateral defection. In the extreme case $(\lambda_i, \lambda_j) = (0, 1)$, the interaction reproduces the classical “sucker” regime of the Prisoner’s Dilemma.

Notably, these dynamics arise under simultaneous decision-making with history-conditioned opponent prediction; exploitation is not an artifact of action-conditioning but a direct consequence of asymmetric valuation. These results show that empathy stabilizes cooperation only under reciprocity. In the absence of symmetry, empathic concern creates predictable vulnerability. This structural tension motivates the adaptive partner-modeling mechanism introduced in Section III F, which enables agents to track and respond to partner asymmetries under exploitation pressure.

C. Implicit communication and recovery dynamics

Beyond equilibrium frequencies, the temporal dynamics of interaction reveal an emergent form of *implicit communication* under high empathy. In our model, agents influence one another solely through their action choices, and their behavior gradually becomes dynamically aligned over time.

Figure 3A and B illustrate these interaction trajectories. In high-empathy regimes, isolated coordination failures such as stochastic defection are followed by rapid recovery to mutual cooperation. The rolling cooperation rate (value of (C, C)) exhibits only brief dips before returning to near unity. In contrast, low-empathy dyads display a qualitatively different pattern: once defection occurs, interactions cascade into persistent mutual defection.

This recovery pattern can be quantified by measuring behavioral synchronization, defined as the fraction of rounds in which both agents select the same action. As shown

in Figure 3C, symmetric high-empathy interactions yield near-perfect synchrony, converging to coordinated cooperation within approximately ten rounds. Low-empathy dyads also synchronize, but on mutual defection. Strongly asymmetric empathy produces persistent desynchronization, reflecting alternating exploitation.

Convergence to the stable regime is similarly rapid under high empathy (Figure 3D). Once cooperation is established, each agent’s Theory of Mind predicts continued partner cooperation, and the empathy-weighted social EFE favors maintaining (C, C) . Because each agent conditions its action on its history-based posterior prediction of the opponent’s behavior, mutual prediction and mutual cooperation form a self-reinforcing loop that stabilizes cooperation against transient perturbations. When an unexpected defection occurs, it increases prediction error and updates beliefs over the opponent’s latent parameters, but under symmetric high empathy this update does not substantially collapse the inferred cooperative disposition of the partner, allowing the dyad to restore cooperation.

From a dynamical systems perspective, this behavior could be interpreted as the emergence of a shared attractor in joint policy space. When both agents weigh the opponent’s welfare, (C, C) minimizes the social EFE for each simultaneously. In this sense, coordination becomes structurally aligned, in the sense that the dyad behaves as if optimizing a partially shared objective rather than two independent payoff functions.

In the standard Prisoner’s Dilemma, mutual defection constitutes the unique Nash equilibrium Kreps (2018) under purely self-regarding utilities Nash (1951), Osborne and Rubinstein (1994). Introducing empathic weighting alters the effective objective function, transforming the stability structure of the interaction and rendering mutual cooperation behaviorally stable under symmetric empathic preferences.

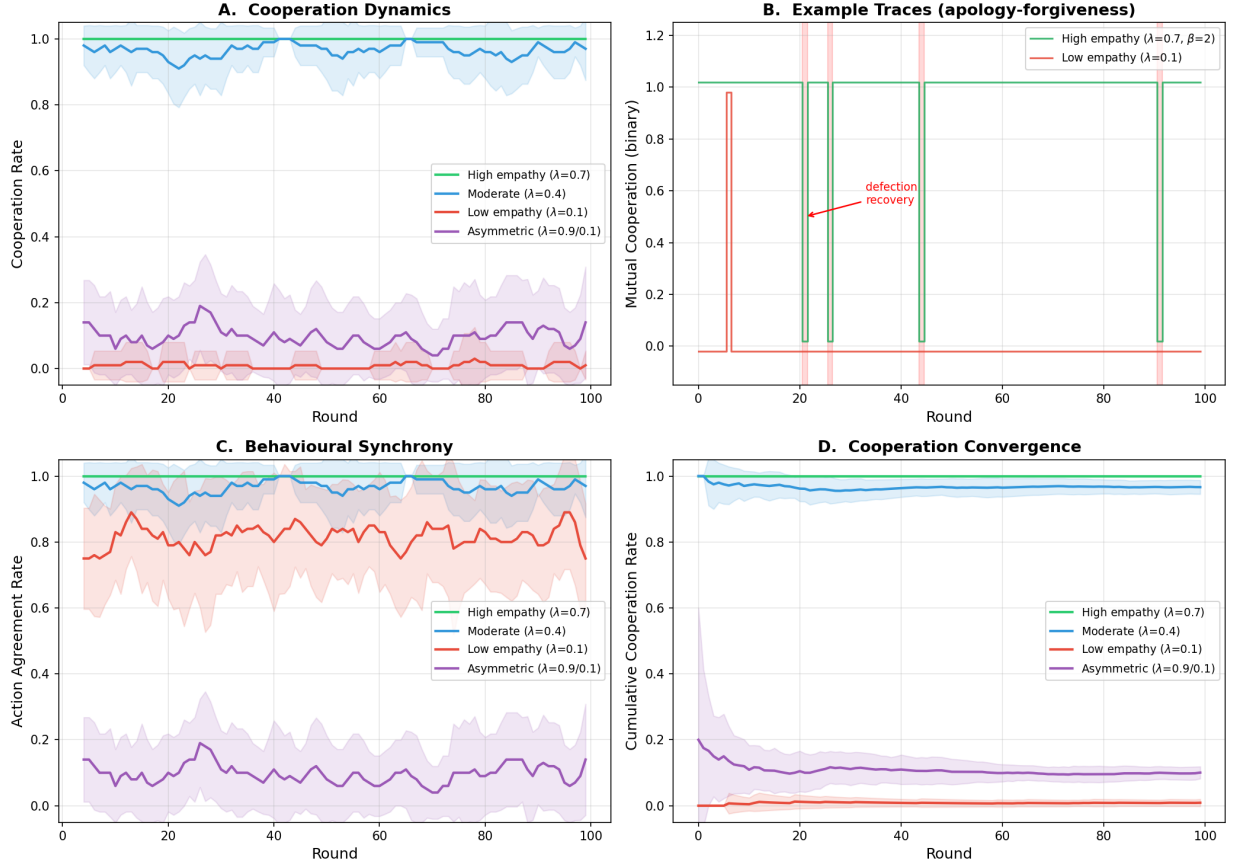


FIG. 3: Temporal cooperation dynamics across empathy regimes. All panels summarize 100-round interactions across simulation seeds under a rolling statistics window of $w = 5$. Shaded bands denote ± 1 standard deviation across seeds. **A:** Rolling mutual cooperation rate. High empathy ($\lambda = 0.7$) rapidly converges to and stabilizes near-perfect cooperation, moderate empathy ($\lambda = 0.4$) sustains cooperation with greater variability, whereas low empathy ($\lambda = 0.1$) and strongly asymmetric empathy ($\lambda = 0.9/0.1$) remain near persistent defection. **B:** Example single-seed trajectories highlighting recovery. Under high empathy, isolated defections are followed by rapid restoration of cooperation (an “apology-forgiveness” pattern), whereas low-empathy agents typically fail to recover once defection occurs. **C:** Rolling action agreement rate, defined as the fraction of rounds in which both agents select the same action (either C, C or D, D). High-empathy dyads synchronize through coordinated cooperation, low-empathy dyads synchronize primarily via mutual defection, and asymmetric empathy yields persistent desynchronization. **D:** Cumulative mutual cooperation rate. High and moderate-empathy dyads converge quickly to sustained cooperative outcomes, while low-empathy and asymmetric interactions converge to trajectories that accumulate few cooperative outcomes.

D. Boundary-layer variability near the transition

To further characterize the boundary between cooperative and exploitative (asymmetric) regimes, we examine interaction dynamics under small empathy asymmetries, focusing on cases where $\lambda_i \approx \lambda_j$, under fixed empathic parameters and without adaptive opponent-parameter updates. Figure 4 illustrates that mean cooperation remains relatively high near symmetry, yet temporal variability increases markedly in this region. In particular, agents exhibit prolonged transients, intermittent defections, and oscillatory coordination patterns before settling into a stable regime.

To quantify this boundary-layer instability, we compute two variability metrics across seeds for each λ_i : (1) the time-averaged width of the rolling cooperation band (band thickness of Figure 4A; mean SD across time), and (2) the seed-to-seed standard deviation of final mutual cooperation frequency (freq_{CC}). We then compare values near the empirical transition region ($\lambda_i \in \{0.20, 0.25, 0.30, 0.35\}$) against higher-empathy configurations well beyond the threshold ($\lambda_i \geq 0.40$).

Variability was significantly elevated near the transition. The mean band thickness was larger by $\Delta = 0.137$ (permutation test, $p = 0.004$), and seed-to-seed outcome variability increased by $\Delta = 0.027$ ($p = 0.0015$). Thus, although average cooperation is already substantial in the near-symmetric region, the interaction dynamics remain statistically less stable than in higher-empathy regimes.

The example trajectories shown in Figure 4B are representative single-seed realizations drawn from these respective groups. They visually illustrate the underlying phenomenon quantified above: near the transition, dyads display extended fluctuations before convergence, whereas far-from-threshold configurations rapidly stabilize into either sustained cooperation or systematic exploitation.

From a dynamical perspective, these findings indicate that the transition region constitutes a boundary layer in which small stochastic perturbations are sufficient to redirect the dyad between competing stable regimes. This variability arises from the deformation of the agents' objective functions under empathy weighting rather than from epistemic exploration per se. Empathy therefore influences not only equilibrium outcomes but also the statistical stability and robustness of coordination.

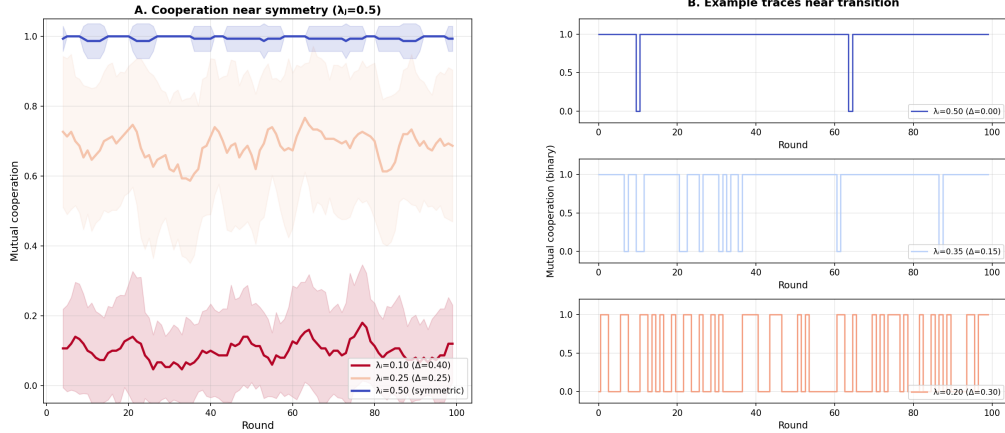


FIG. 4: **Boundary-layer dynamics near empathy symmetry** ($\lambda_j = 0.5$). **A**: Rolling mutual cooperation rate (window $w = 5$, mean ± 1 SD across seeds) for varying λ_i . While mean cooperation remains high close to symmetry, variability increases sharply near the cooperation-exploitation threshold. This indicates reduced dynamical stability despite similar equilibrium levels of cooperation. **B**: Representative single-seed trajectories illustrating the underlying temporal structure. Near the transition, interactions show more frequent defections.

These signatures suggest the presence of an underlying transition in the stability structure of the dyadic interaction. We therefore make this transition explicit by defining and analytically characterizing the cooperation threshold as a function of empathic weighting.

E. Transition to cooperation

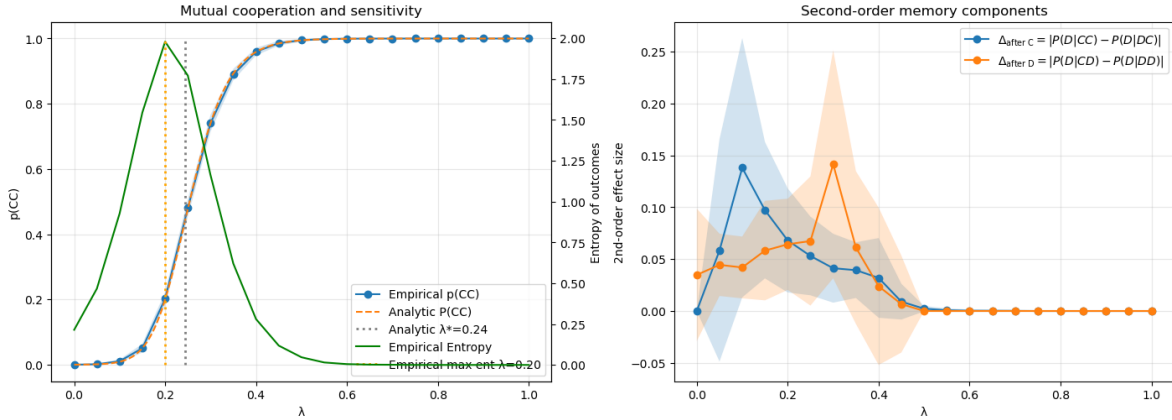


FIG. 5: **Transition to cooperation.** **Left:** Empirical and analytical probability of mutual cooperation as a function of λ . The transition point $\lambda \approx 0.24$ is the point of maximal sensitivity of the distribution, which is greater than the point of maximal uncertainty about the cooperation outcome (maximal entropy of the sequences). The transition point is exactly $\lambda = 0.2$ in the deterministic limit. **Right:** Memory effects for an individual agent measures as conditional probability rates with respect to the agent’s history. At the boundaries of the transition point, there are peak memory effects (second order conditioning) in which defection is stubborn ($\lambda \approx 0.1$), or the cooperation is fragile ($\lambda \approx 0.35$) for a single agent. This effect is due to the coupling with the other agent.

The cooperation landscape in Figure 1 and the near-symmetric trajectories in Figure 4 indicate a sharp, threshold-like shift from predominantly defective play to sustained mutual cooperation as empathic weighting increases. We quantify this transition by fixing the partner at $\lambda_j = 0.5$ and sweeping λ_i across the boundary region. Table I reports the resulting mutual cooperation frequency freq_{CC} across seeds. Unless otherwise specified, the results in this subsection are obtained under fixed empathic parameters and without opponent-parameter inference, isolating the pragmatic contribution of empathic weighting to cooperation dynamics.

Two features stand out from Table I. First, the transition is strongly asymmetric. Cooperation is fragile to empathic *deficit*. Reducing λ_i from 0.50 to 0.20 collapses mutual cooperation from 99.5% to 44.3%, and variability peaks near the boundary (Std CC ≈ 0.052 at $\lambda_i = 0.20$). Second, cooperation rapidly saturates under empathic *excess*. Increasing λ_i

TABLE I: Cooperation transition with $\lambda_j = 0.5$ ($T = 100$, 30 seeds).

λ_i	Mean CC	Std CC
0.10	0.101	0.034
0.20	0.443	0.052
0.25	0.686	0.045
0.30	0.859	0.029
0.35	0.942	0.016
0.40	0.979	0.014
0.45	0.990	0.010
0.50	0.995	0.008
≥ 0.55	~ 0.997	~ 0.006

above ≈ 0.45 yields only marginal gains, consistent with a ceiling effect once (C, C) becomes the dominant attractor of the interaction.

This asymmetry is practically relevant for multi-agent design. The minimum empathic weighting required to reliably sustain cooperation can be substantially below $\lambda = 1$, but performance is brittle near the boundary, where small decreases produce disproportionately large drops in freq_{CC} . Importantly, this sharp empirical boundary suggests an underlying change in the stability structure of the dyadic decision process. We next formalize this transition by analyzing the dyadic cooperation probability $P(CC)(\lambda)$ and defining the transition point λ^* via maximal sensitivity, linking the empirical sweep to the analytical characterization in Figure 5.

To further investigate the transition to the mutual cooperation attractor in the IPD, with payoff function $u_j(a_i, a_j)$ for $i, j \in 0, 1$, we study the probability of mutual cooperation $P(CC)(\lambda)$ as a function of the control parameter λ . Using (13) and (7), the probability of cooperation for agent i is

$$P_i(C) = \sigma(\beta\Delta U(\lambda)), \tag{22}$$

with $\Delta U(\lambda) = U(C, \lambda) - U(D, \lambda)$ and $U(a_i) = (1 - \lambda)q(a_j|a_i)u_i(a_i, a_j) + \lambda q(a_j|a_i)u_j(a_i, a_j)$ for a given opponent action a_j . Here $\sigma(x) = 1/(1 + \exp(x))$. Assuming $\beta_s = \beta_o = \beta$, and

identical, independent agents (without learning or inversion), we obtain

$$P(CC) = P_i(C)P_j(C) = p^2(\lambda, \beta). \quad (23)$$

We define the transition point as the value of λ at which $P(CC)$ is most sensitive to changes, that is, where $P''(CC) = 0$. Under these conditions, the transition point is given by

$$\lambda^* = \frac{\ln 2/\beta - A}{B}, \quad (24)$$

with $A = q_0R + (1 - q_0)S - q_1T - (1 - q_1)P$, $B = (T - S)(1 - q_0 + q_1)$, and $q_0 \equiv q(C|C)$, $q_1 \equiv q(C|D)$. Here T, R, S, P denote the payoff values of the IPD. Note that $p(\lambda^*) = 2/3$, indicating that the dyad is most sensitive to parameter changes when cooperation is already relatively high. The corresponding distributions for the payoff structure used in this paper are shown in Figure 5, left. In the deterministic limit $\beta \rightarrow \infty$, the transition point occurs at $\lambda = 0.2$, which corresponds to the point of maximal entropy (indifference). This point of maximal indifference (entropy) in the action sequences is surrounded by increasing bouts of cooperation, leading to two distinct types of apparent memory effects at the individual-agent level. For lower values of empathy, $\lambda \approx 0.1$, agents display *stubborn defection*: even after choosing cooperation, they remain more likely to defect. Conversely, for higher values of empathy, $\lambda \approx 0.35$, agents exhibit *fragile cooperation*, where a single defection increases the likelihood of subsequent defections.

F. Learning improves belief accuracy but does not induce cooperation

To disentangle the role of belief accuracy from that of social valuation, we evaluate learning-enabled variants in which each agent maintains a particle filter posterior over continuous opponent parameters $\theta_j = (\alpha, \rho, \beta, \lambda_j)$, representing cooperation bias, reciprocity sensitivity, behavioral precision, and empathic weighting, respectively. Rather than inferring discrete strategy types, the agent performs online Bayesian inference over this parametric behavioral profile.

Figure 6, parts A and B, show the evolution of inferred opponent parameters over repeated interaction. When facing a cooperative partner ($\lambda_j = 0.7$), the posterior mean of α converges to a strongly positive value, indicating persistent cooperative bias, while reciprocity (ρ) and precision (β) stabilize with decreasing uncertainty. When facing a low-empathy partner

($\lambda_j = 0.1$), α converges to a negative value, reflecting sustained defection, and the posterior contracts rapidly. In both cases, uncertainty bands shrink over time, demonstrating well-calibrated and convergent belief formation.

Improved opponent modeling does not increase cooperation. Figure 6C compares cooperation rates under static Theory of Mind and learning-enabled inference. At low empathy ($\lambda_i = 0.2$), learning slightly reduces mutual cooperation. Identifying the partner as reliably cooperative sharpens the expected payoff gradient favoring defection, reducing mutual cooperation from 45.0% (static ToM) to 43.2% (learning-enabled). A similar effect appears at $\lambda_i = 0.3$, where cooperation decreases from 87.0% to 85.6%. Only when empathy is sufficiently high ($\lambda_i \geq 0.5$) does cooperation remain near ceiling regardless of whether learning is active.

These results demonstrate a structural dissociation between epistemic inference and prosocial valuation. Learning refines the agent’s posterior over opponent parameters, increasing predictive precision, but cooperation is governed by empathic weighting in the social EFE. Accurate belief alone does not induce cooperation; it can instead sharpen exploitation when empathic concern is weak. Cooperation therefore arises from the deformation of the agent’s objective under λ , not from opponent classification or reciprocal expectation.

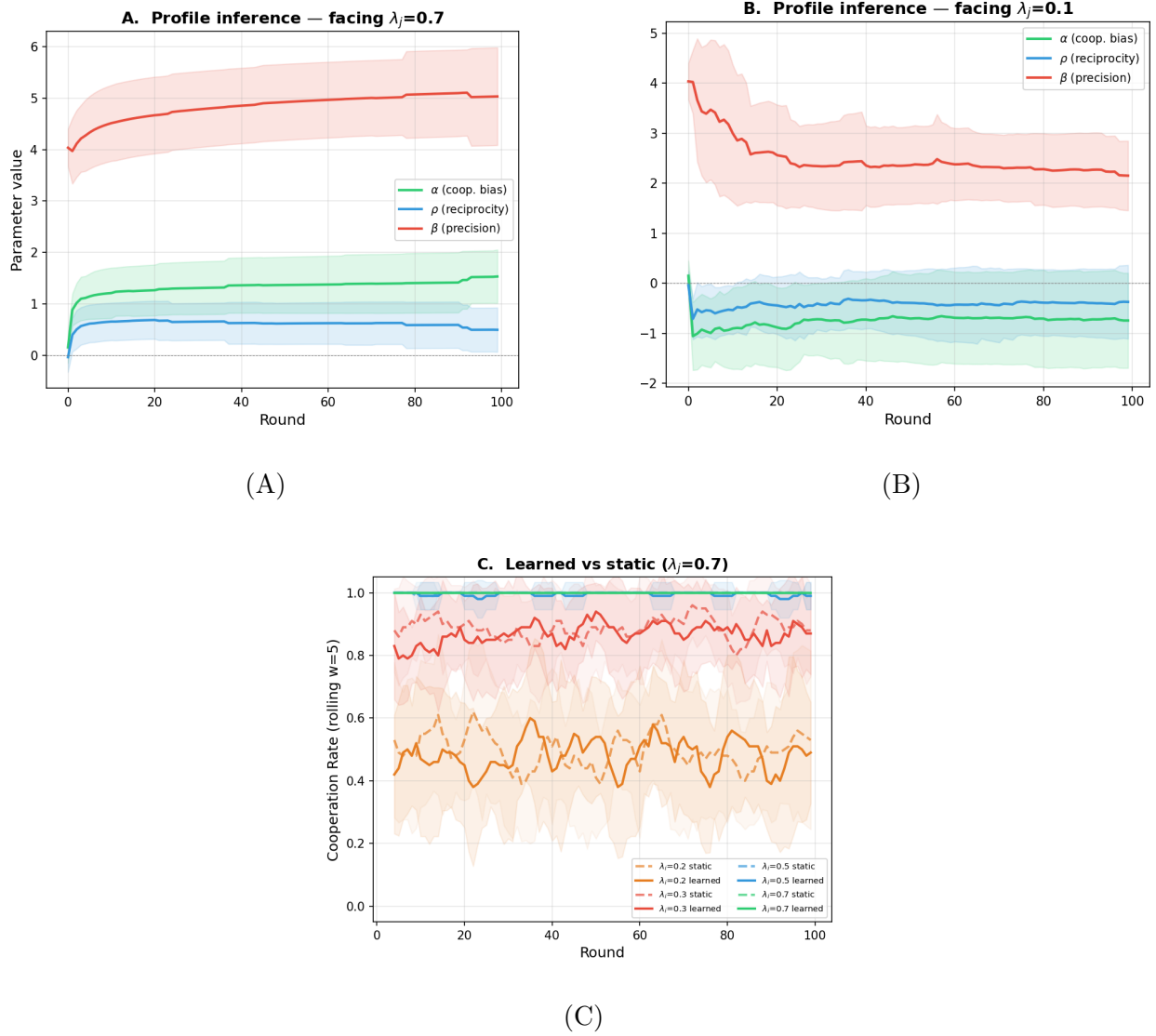


FIG. 6: **Opponent parameter inference and its effect on cooperation.** **A:** Posterior mean and uncertainty (shaded bands) over opponent behavioral parameters (α, ρ, β) when facing a cooperative partner ($\lambda_j = 0.7$). The cooperation bias parameter α converges to a strongly positive value, with uncertainty contracting over time. **B:** Parameter inference when facing a low-empathy partner ($\lambda_j = 0.1$). The inferred cooperation bias α converges negative, reflecting sustained defection. In both cases, posterior uncertainty decreases monotonically, indicating stable convergence of the particle filter. **C:** Cooperation rate under learning-enabled inference (solid lines) versus static Theory of Mind (dashed lines). While learning improves belief accuracy, it does not increase cooperation. At low empathy, more precise inference slightly increases exploitation, reducing mutual cooperation. At high empathy, cooperation remains near ceiling regardless of learning.

TABLE II: Cooperation rate by planning horizon (symmetric empathy, $T = 100$, 20 seeds).

λ	$H = 1$	$H = 2$	$H = 3$	$\Delta(H3-H1)$
0.1	0.014	0.032	0.038	+0.024
0.2	0.255	0.257	0.258	+0.002
0.3	0.782	0.657	0.597	-0.185
0.4	0.970	0.873	0.788	-0.182
0.5	0.997	0.952	0.886	-0.111
0.7	1.000	0.995	0.965	-0.035

G. Strategic sophistication amplifies the need for empathy

All results presented thus far were obtained under myopic action selection ($H = 1$), in which agents evaluate only the immediate social EFE of each candidate action. We now ask whether increasing strategic sophistication, operationalized as multi-step planning, enhances or undermines cooperation.

To this end, we compare myopic agents against sophisticated agents that enumerate all 2^H candidate policies over planning horizons $H = 2$ and $H = 3$, evaluating each policy via forward rollout (described in Section II). At rollout step t , the partner’s predicted response is computed using the gated history-conditioned Theory of Mind prediction at $t = 0$ and the static history-conditioned prior for $t > 0$, as no new observations are available during planning.

The policy-level social EFE is averaged across the horizon as:

$$G(\pi) = \frac{1}{H} \sum_{t=0}^{H-1} \left[(1 - \lambda)G_{\text{self}}^{(t)} + \lambda G_{\text{other}}^{(t)} + G_{\text{epistemic}}^{(t)} \right]. \quad (25)$$

and actions are selected by marginalizing the softmax posterior $Q(\pi) \propto \exp(-\beta G(\pi))$ to the first time step. All other parameters were held constant.

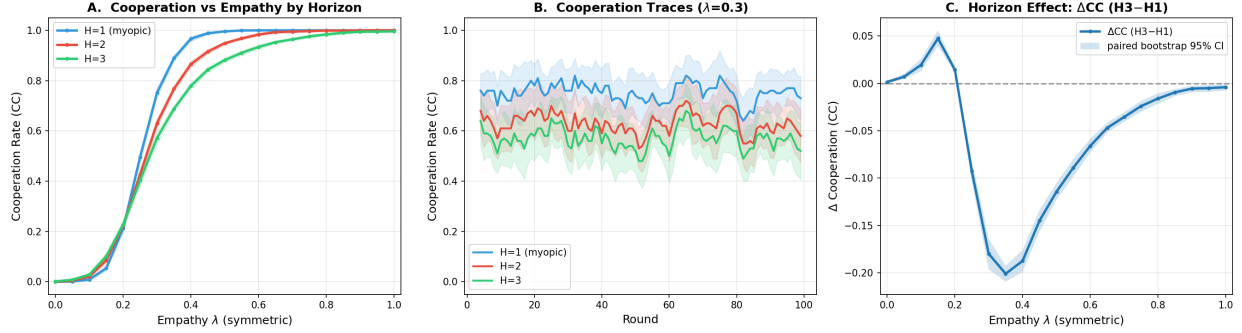


FIG. 7: **Cooperation rates across empathy levels and planning horizons.** **A:** Cooperation rate as a function of symmetric empathy ($\lambda_i = \lambda_j$) for planning horizons $H = 1$ (myopic), $H = 2$, and $H = 3$. Increasing planning depth shifts the cooperation curve rightward, raising the empathy threshold required to sustain cooperation. **B:** Rolling cooperation rate at $\lambda = 0.3$, near the transition region. Shaded regions denote 95% confidence intervals of the mean across 20 seeds. Myopic agents maintain substantially higher cooperation than multi-step planners. **C:** Horizon effect quantified as $\Delta CC(\lambda) = CC_{H3} - CC_{H1}$ with paired bootstrap 95% confidence intervals. Multi-step planning slightly increases cooperation at very low empathy, but substantially decreases cooperation in the intermediate regime ($\lambda \approx 0.3\text{--}0.5$), before converging toward zero effect at high empathy.

Table II and Figure 7 summarize the results under symmetric empathy ($\lambda_i = \lambda_j$). Contrary to the intuition that greater foresight should stabilize cooperation, we find that increasing planning depth systematically reduces cooperation at moderate empathy levels. At $\lambda = 0.3$, extending the horizon from $H = 1$ to $H = 3$ decreases mutual cooperation from 78.2% to 59.7% ($\Delta CC = -0.185$, 95% bootstrap CI $[-0.200, -0.171]$; paired sign-flip permutation test $p < 10^{-4}$, 20 seeds). The reduction is strongest in the transition region ($\lambda = 0.3\text{--}0.4$). At $\lambda = 0.4$, cooperation drops from 97.0% to 78.8% ($\Delta CC = -0.181$, CI $[-0.193, -0.169]$; $p < 10^{-4}$), closely matching the largest observed decrease at $\lambda = 0.3$. A smaller but still reliable drop persists even near ceiling cooperation ($\lambda = 0.5$: 99.7% to 88.6%, $\Delta CC = -0.112$, CI $[-0.121, -0.102]$; $p < 10^{-4}$).

The horizon effect is not monotone in λ . At very low empathy, longer horizons produce a small increase in cooperation (Figure 7C): $\lambda = 0.1$ yields $\Delta CC(H3 - H1) = 0.024$ (CI $[0.018, 0.031]$; $p < 10^{-4}$). At $\lambda = 0.2$, however, the effect is negligible and not statistically reliable ($\Delta CC = 0.002$, CI $[0.000, 0.004]$; $p = 0.125$). At high empathy, cooperation remains

near ceiling across horizons, and the decrement becomes comparatively modest ($\lambda = 0.7$: $\Delta CC = -0.035$, CI $[-0.040, -0.031]$; $p < 10^{-4}$). Overall, sophisticated planning most strongly undermines cooperation in the boundary region where cooperation is feasible but not yet guaranteed.

Under myopic evaluation, agents compare immediate payoffs: cooperation yields $R = 3$ (or $S = 0$ if exploited), whereas defection yields $T = 5$ (or $P = 1$). With sufficient empathy, the opponent-welfare term in the social EFE offsets the temptation payoff, stabilizing cooperation. Under multi-step planning, however, the temptation advantage compounds across the horizon. A defection-initial policy can harvest the temptation payoff at $t = 0$ and anticipate favorable downstream consequences, making defection-initial policies increasingly attractive as H grows. In effect, planning amplifies the cumulative advantage of temptation over cooperation, shifting the cooperation curve rightward (Figure 7A).

We quantify this rightward shift via a threshold definition $\lambda^* = \min\{\lambda : \mathbb{E}[CC] \geq 0.8\}$. Under this criterion, the cooperation threshold increases discretely with horizon, from $\lambda^* = 0.35$ for $H = 1$ to $\lambda^* = 0.40$ for $H = 2$ and $\lambda^* = 0.45$ for $H = 3$ (bootstrap medians; $\Delta\lambda^*(H3 - H1) = 0.10$ on the λ grid used in the sweep). Thus, greater strategic foresight increases the empathic weighting required for reliably cooperative play.

This result parallels the classical backward-induction argument in the IPD, in which perfectly rational agents unravel cooperation entirely (Osborne and Rubinstein 1994). In the present framework, planning does not eliminate cooperation, because empathy provides a countervailing valuation of the partner’s welfare. However, increased planning depth systematically strengthens the strategic pressure toward defection unless empathy is sufficiently strong to counterbalance it.

These findings highlight a structural distinction between *capability* and *alignment*. Increasing planning depth enhances strategic capability but does not increase prosocial valuation. Indeed, without corresponding empathic weighting, greater capability can undermine cooperation by magnifying the long-horizon benefits of exploitation. Cooperation in this framework is therefore a consequence of value alignment embedded in the social EFE.

In conclusion, myopic planning and empathy emerge as complementary mechanisms: myopic agents cooperate more readily because they do not anticipate future temptation, whereas sophisticated agents require stronger empathic motivation to resist the compounded lure of defection. This distinction has direct implications for AI alignment: increasing an

agent’s planning capacity without strengthening its prosocial valuation may reduce cooperative behavior, formalizing the concern that more capable systems can be harder to align.

H. Phase transition-like dynamics in the system

Treating λ as a control parameter and mutual cooperation as an order parameter, the sharp rise to a threshold in mutual cooperation as λ passes a certain critical value resembles a phase transition. Indeed, there are several classic signatures of finite-size transitions. Defining λ^* by maximal sensitivity provides a susceptibility peak for the derivative of $P(CC)$ with respect to λ . As shown in Fig. 4, elevated variability near the transition point was observed, a boundary-layer instability where small perturbations can redirect trajectories between competing attractors, resembling divergence of correlation near the critical point. Finally, the long transients near the boundary provide a finite-size analogue of critical slowing. Note also that the determining property of one phase or another is that of the minimisation of variational free energy in the control parameter, another feature of a phase transition.

The form of

$$P_i(C) = \sigma(\beta\Delta U(\lambda))$$

makes it a logit choice rule with precision β and utility gap $\Delta U(\lambda)$. On that view, the transition is a regime change or equilibrium-selection crossover driven by the parameter λ deforming effective utilities.

Alternatively, the model maps to a spin in a field under Glauber dynamics: actions C or D are spins up or down, β is an inverse temperature, and $\Delta U(\lambda)$ is (twice) the effective local field, such that the order parameter (what one would think of as magnetisation) is

$$m = \tanh(\beta\Delta U(\lambda)/2)$$

with $P(C) = (1 + m)/2$, so that $P(CC)$ is the square (under independence). In the limit of infinite β , \tanh will become a *signum* function, producing a sharp switch at the point where $\Delta U(\lambda) = 0$.

However, note that at finite precision, the analytic form of $P_i(C)$ is logistic, meaning there is no non-analytic behaviour as expected from a true phase transition.

A true thermodynamical phase transition needs a large system and a self-consistency condition. Since the dyad already has a coupling mechanism and a noisy bistability property,

it would be interesting in future work to investigate what happens when many agents are considered, or an explicit mean field coupling through group interaction is introduced.

IV. DISCUSSION

A. Relation to active inference literature

The proposed empathy-driven cooperation mechanism builds on multiple strands of work in the active inference literature, particularly research on social interaction, games, and multi-agent coordination. One important foundation is active inference applied to strategic games and social dilemmas. Demekas et al. (2023) introduced a mathematically tractable active inference formulation of the Iterated Prisoner’s Dilemma, demonstrating how agents can learn adaptive responses over repeated interactions. In that formulation, however, agents reason over the joint state space of the game, enumerating possible action combinations, without maintaining distinct internal models of one another. Our work extends this line by endowing each agent with an explicit Theory of Mind module that predicts the opponent’s behavior from interaction history (and, during rollouts, from simulated history), and a social EFE that directly weights the opponent’s welfare, providing a step toward more cognitively grounded multi-agent active inference.

Relatedly, Pitliya et al. (2025), Çatal et al. (2024) proposed a factorised active inference framework for multi-agent interactions, in which agents maintain explicit beliefs about others’ internal states and preferences. Our approach is broadly congruent with this factorised perspective. Each agent maintains a separate generative model of the opponent (the “other-model”) alongside its own self-model, and uses the other-model to simulate the opponent’s expected free energy when evaluating candidate actions. The key innovation is that cooperation emerges not from learned reciprocity or centralised coordination, but from the structural weighting of the opponent’s welfare in the social EFE through the empathy parameter λ . The emergent alignment observed in our simulations, manifested as behavioural synchronisation and stable mutual cooperation, can thus be interpreted as an active inference realisation of shared belief states and generalised synchrony between interacting agents, arising from the shared mathematical structure of empathic EFE minimisation.

Our model also connects naturally to neuroscience-inspired active inference accounts of

the Theory of Mind and second-person interaction. Recent work has argued that active inference is particularly well suited to capturing the dynamics of social cognition, including mutual awareness, coordination, and reciprocal adaptation. For example, Lehmann et al. (2024) describes how second-person neuroscience can be formalised as coupled active inference processes exchanging signals over time. In our setting, such exchanges are abstracted to the observation of joint outcomes, yet these observations are sufficient to induce coupling between internal belief states through the ToM prediction mechanism. The use of two generative models with shared structure, one self-oriented and one modelling the opponent, parallels Bayesian interpretations of the mirror neuron system, according to which similar hierarchical models support both action execution and action observation.

This mechanism aligns with the view of active inference as a drive toward cognitive consistency Friston (2018), wherein agents minimise dissonance between predicted and observed actions of self and others. The empathic agent operationalises this principle by incorporating the opponent’s expected free energy directly into its own action evaluation. In doing so, the agent moves toward outcomes that minimise surprise for both agents simultaneously, corresponding to a form of empathic alignment or phenomenological isomorphism. From the perspective of ethical AI, such alignment via empathy offers a plausible route toward human-compatible systems, insofar as artificial agents come to treat human goals as internally salient during planning rather than as externally imposed constraints.

Our results further clarify the relationship between empathic weighting and learning-based reciprocity. In a learning-enabled variant that performs Bayesian inference over opponent behavioural parameters (cooperation bias, reciprocity, precision) and latent empathic weighting via a particle filter, opponent models converge rapidly and accurately, yet cooperation remains primarily determined by the empathy parameter λ . Accurate belief that the opponent will cooperate actually *increases* the temptation to exploit at low empathy, slightly reducing cooperation. This demonstrates that the cooperative behaviour observed here is not reducible to learned best-response strategies or reciprocation alone, but is instead induced by the structural commitment to weighting the opponent’s welfare in the social EFE. In this sense, empathy functions as a prior over social valuation that shapes equilibrium selection and coordination stability, while learning primarily refines the accuracy of opponent predictions without altering the fundamental cooperation mechanism. Moreover, by treating the opponent’s empathic weighting as a latent variable, the framework supports a

genuine epistemic term in expected free energy, yielding principled exploratory behaviour (e.g., early cooperation as information-seeking) that is not reducible to standard Boltzmann rationality.

The sophisticated inference results reveal an additional and somewhat counterintuitive insight. Increasing planning depth *reduces* cooperation at moderate empathy levels. Extending the planning horizon from $H = 1$ (myopic) to $H = 3$ shifts the cooperation threshold rightward, from approximately $\lambda \approx 0.25$ to $\lambda \approx 0.45$. This occurs because forward-looking agents can anticipate the cumulative temptation payoff over multiple steps, making defection-initial policies more attractive in the social EFE landscape. Only agents with sufficiently high empathy ($\lambda \gtrsim 0.7$) resist this temptation regardless of planning depth. This finding parallels the well-known backward-induction argument in finitely repeated games, where perfectly rational agents unravel cooperation entirely (Osborne and Rubinstein 1994). In our framework, the unravelling is graded rather than complete, because the empathy term provides a countervailing force that increases with λ . The practical implication is that planning capability and prosocial motivation must scale together: increasing an agent’s lookahead without a corresponding increase in empathy may paradoxically reduce cooperative behaviour.

A further implication of the present results is that empathy affects not only equilibrium outcomes but also transient dynamics near regime boundaries. In the Iterated Prisoner’s Dilemma, small empathy asymmetries and near-symmetric settings can exhibit long transients, oscillations, and elevated variance before settling into stable cooperation or exploitation. Such variance amplification near the transition is consistent with critical phenomena near bifurcations¹, where competing policies have comparable expected free energy and stochasticity induces intermittent switching. This highlights that empathic inference modulates the reliability and temporal structure of coordination, not merely the mean cooperation rate, and motivates analysis of stability and transient behaviour as first-class targets for evaluation.

¹ We emphasize that this is a phase-transition analogy (a finite-size crossover) rather than a true thermodynamic phase transition.

B. Benefits and limitations

A primary advantage of the proposed framework is its conceptual transparency and modularity. The social EFE formulation $G_{\text{social}} = (1 - \lambda)G_{\text{self}} + \lambda G_{\text{other}}$ provides a single, interpretable control parameter (λ) that governs the degree of prosocial behaviour. This simplicity facilitates analysis: the cooperation threshold, exploitation dynamics, and planning-depth effects can all be understood in terms of how λ shifts the balance between self-interest and opponent welfare in the EFE landscape. The modular architecture, separating state inference, opponent modelling (ToM and particle filter), and action selection (myopic or sophisticated), allows each component to be evaluated and improved independently.

The opponent modelling pipeline offers additional practical benefits. The particle filter provides interpretable, online Bayesian inference over opponent profiles, and the reliability-gated blending between learned and static ToM predictions ensures graceful degradation. When insufficient data has been collected, the agent falls back to a reasonable prior rather than acting on unreliable inferences. This design pattern “trust your model only when it has earned trust” is broadly applicable to multi-agent systems where partner behaviour is initially unknown.

The behavioural consequences of this design are also significant. Empathic agents exhibit robust and ethically desirable behaviour, in part because they internally simulate the consequences of their actions on others through the opponent welfare term in the social EFE. In our experiments, this manifested as resistance to short-term exploitative strategies and a sustained commitment to cooperation when empathy was mutual. Such properties are attractive for real-world AI systems, as they may mitigate power-seeking or opportunistic behaviour by making harmful outcomes salient within the agent’s own planning dynamics.

Nevertheless, several limitations warrant attention. First, the Theory of Mind module currently uses a static, history-conditioned payoff-based prediction of opponent responses. While the particle filter learns opponents’ behavioural characteristics, the per-step opponent prediction during sophisticated planning rollouts ($t > 0$) relies on the static ToM prior, since no new observations are available during mental simulation. More sophisticated approaches, such as recursive ToM, where the opponent is modelled as itself performing ToM about the agent, could improve the fidelity of multi-step predictions, though at substantially increased computational cost.

Second, the present implementation relies on discrete state spaces with relatively low dimensionality, and similar models. The Prisoner’s Dilemma, with its four joint outcomes and two actions, is an ideal testbed for validating the core mechanism, but scaling to richer environments with continuous states, high-dimensional observations, heterogeneous models, and larger action spaces raises well-known challenges associated with policy enumeration and belief propagation. In the sophisticated planning regime, the number of candidate policies grows as 2^H , which becomes prohibitive for large horizons. Approximate inference schemes, such as Monte Carlo tree search or amortised policy networks, may be required for more complex settings. The ultimate goal is to be able to model agents with disparate models and still enable a degree of theory of mind and empathy.

The empathy parameter λ is currently fixed for each agent throughout an interaction. In human social cognition, empathy is modulated dynamically based on context, relationship history, and emotional state. While our reliability-gated opponent modelling provides some adaptive modulation of *beliefs* about the opponent, the degree of prosocial *concern* (λ) remains static. Extending the framework to allow online inference over λ , for instance, by treating empathy as a latent variable with its own generative model, would enable agents to dynamically adjust their prosocial commitment in response to partner behaviour, potentially capturing phenomena such as empathy fatigue and strategic withdrawal.

Finally, the ethical implications of powerful social modelling must be carefully considered. The same capacities that enable an agent to cooperate effectively could also enable manipulation. An agent that accurately models another’s preferences and predicts their responses could exploit this knowledge for self-serving ends when empathy is low. Our results demonstrate this directly: low-empathy agents with accurate opponent models exploit cooperative partners. Safeguards drawn from AI safety research, including alignment evaluation protocols and controlled deployment environments, should therefore accompany the development of socially capable agents.

C. Empathy, exploitation, and the motivational gap

The results above raise a question that the present framework can pose but not yet resolve. What separates computational empathy from genuine empathic concern?

The dissociation is already visible in our own data. The learning results (Section III F)

show that an agent with accurate posterior beliefs about opponent parameters but low λ does not cooperate more; it exploits more effectively. The sophisticated planning results (Section III G) sharpen this. Greater cognitive capability without corresponding empathic weighting actively undermines cooperation. In both cases, the cognitive machinery (ToM, planning) and the empathic weighting (λ) contribute independently to behavior. The architecture makes this separation explicit; the ToM module predicts what the opponent will do (via history-conditioned posterior prediction), while λ determines whether the opponent’s welfare enters the agent’s own objective (via the social EFE).

The cognitive science literature documents precisely this pattern. Intact social modeling capacity paired with absent prosocial concern, a profile characteristic of instrumental empathy, in which perspective-taking serves manipulation rather than mutual benefit Shamay-Tsoory et al. (2009), Breithaupt (2019). The alignment implication is direct. If accurate social modeling can serve exploitation just as readily as cooperation, then equipping agents with sophisticated ToM is not sufficient for alignment. What matters is the motivational structure that determines how social knowledge is used; in our framework, the question of what sets λ .

In the present model, λ is fixed exogenously. A design choice that isolates the effect of empathic weighting from confounding variables. But in cognitive science, empathy is increasingly understood as a motivated capacity, dynamically regulated based on context, expected costs, and social goals rather than deployed uniformly Spaulding (2024), Zaki (2014). An agent in a cooperative regime has reason to invest in allocentric modeling because it reliably reduces prediction error; an agent facing exploitation has reason to withdraw. Within active inference, this regulation maps onto precision dynamics. When allocentric predictions reliably improve model fit, their precision increases and empathic inference is upregulated; when the social environment turns adversarial, precision drops and the agent reverts toward egocentric processing. The trust-gating mechanism shown in Section II D, Eq. (13) already implements a version of this logic for opponent modeling. Extending it to govern the empathy parameter itself, treating λ as inferred rather than fixed, would allow the degree of prosocial concern to emerge from interaction dynamics.

Such an extension, however, would not by itself ensure prosociality. Precision optimization is motivationally neutral. It determines when social modeling is useful, not whether it will be used for cooperation or exploitation. Addressing this gap likely requires agents

with richer motivational architectures, systems in which prosocial behavior is grounded in something analogous to social urges (e.g., affiliation demands) whose satisfaction depends structurally on the welfare of interaction partners Bach (2012). Integrating such motivational structure with active inference represents a natural next step toward agents whose empathy is not merely a parameter but a consequence of their own need dynamics.

D. Future directions

Several avenues for future work naturally follow from this framework. On the modelling side, the most immediate extension is the recursive Theory of Mind, in which the opponent is modelled as itself performing ToM about the agent. The current architecture supports depth-1 ToM (if I do a_i , opponent responds with a_j); extending to depth-2 (opponent anticipates my response to their action) would enable richer strategic reasoning. Preliminary architectural support for this exists in the codebase via the `DepthTwoToM` class, but empirical evaluation of its effects on cooperation dynamics remains for future work. In the same vein, a future research avenue entails looking into heterogeneous models, and degrees of overlap to see how we can instantiate theory of mind.

A second promising direction involves adaptive empathy. Rather than fixing λ as a static parameter, it could be treated as a latent variable inferred online from interaction outcomes. An agent that observes persistent exploitation could reduce its effective empathy, implementing a principled form of empathy withdrawal that balances prosocial concern with self-protection. Conversely, an agent that observes reciprocated cooperation could increase its empathy, reinforcing cooperative dynamics. Such a mechanism would bridge the gap between empathy-based and reciprocity-based accounts of cooperation by allowing empathy itself to be shaped by experience.

A third direction concerns scaling beyond dyadic interaction. The current framework considers two-player interactions, but many real-world coordination problems involve groups. Extending the social EFE to N agents, for instance, as $G_{\text{social}} = (1 - \lambda)G_{\text{self}} + \frac{\lambda}{N-1} \sum_{j \neq i} G_{\text{other}_j}$ raises questions about computational tractability, the emergence of in-group/out-group dynamics, and the stability of cooperation at scale. Preliminary theoretical considerations suggest that pairwise empathic alignment may generalise to group-level coordination, but understanding the conditions under which such dynamics remain stable

and fair at societal scales represents an important frontier. This would also require moving from separate generative models to a sub-tensor architecture wherein the same model is simply parameterized by a context factor.

On the computational side, the sophisticated planner’s 2^H policy enumeration becomes intractable for large horizons. Integrating Monte Carlo tree search, neural amortisation of policy evaluation, or hierarchical planning over temporally abstracted options could extend the effective planning horizon without exponential cost growth. Additionally, implementing the framework on neuromorphic hardware could enable real-time empathic inference in embodied agents, such as social robots that adapt their behaviour based on ongoing inference about human states and intentions.

Finally, empirical validation in richer environments is essential. Testing empathic agents in more complex multi-agent simulations, such as public goods games, negotiation tasks, or cooperative construction, and in human-AI interaction studies would provide critical insight into the framework’s robustness and social impact. Cooperative human-AI games could assess whether empathic inference improves trust, satisfaction, and coordination relative to non-empathic baselines, providing empirical grounding for the theoretical claims advanced here.

V. CONCLUSION

We have presented a framework for implementing empathy in artificial agents within the active inference paradigm, centred on the social EFE: $G_{\text{social}} = (1-\lambda)G_{\text{self}} + \lambda\mathbb{E}[G_{\text{other}}]$. We endowed each agent with a Theory of Mind module that predicts the opponent’s response to candidate actions, and weighting the opponent’s expected free energy alongside the agent’s own, and thus introduced a mechanism for prosocial behaviour that requires no hand-crafted social rules, explicit communication, or centralised coordination. Cooperation emerges as a natural consequence of empathic planning. Agents that weigh the opponent’s welfare prefer outcomes that benefit both parties, shifting the equilibrium from mutual defection to mutual cooperation.

Our results in the Iterated Prisoner’s Dilemma reveal several key findings. First, cooperation exhibits a sharp phase transition as a function of empathy, with a critical threshold near $\lambda \approx 0.25$ under myopic planning and $\lambda \approx 0.45$ under sophisticated multi-step planning. Sec-

ond, empathy asymmetries systematically produce exploitation, with low-empathy agents extracting higher payoffs from high-empathy partners. Third, Bayesian opponent modelling via particle filtering provides accurate and convergent inference over opponent profiles, but cooperation is driven by the empathy parameter rather than by learned beliefs. Accurate knowledge that the opponent cooperates is not sufficient to sustain cooperation without sufficient prosocial motivation. Fourth, and perhaps most strikingly, increasing planning depth reduces cooperation at moderate empathy levels, demonstrating that rationality and cooperation are in tension absent sufficient empathic weighting. This last finding carries a direct implication for AI alignment: increasing an agent’s planning capability without a commensurate increase in prosocial motivation may paradoxically make the agent less cooperative.

These results highlight the promise of active inference as a foundation for socially aligned artificial intelligence. An agent that models others’ beliefs, goals, and welfare, and incorporates that understanding into its own planning, is better positioned to coordinate, respect others’ interests, and avoid harmful strategic behaviour. More broadly, this work points toward a class of AI systems that are not only capable of intelligent action but also sensitive to the social and ethical dimensions of interaction. The active inference paradigm offers a principled unifying framework for this endeavour, integrating perception, action, learning, and social cognition under a single information-theoretic formalism. By combining insights into human empathy with Bayesian modelling and multi-step planning, we move closer to artificial agents that participate meaningfully in human social environments, agents that cooperate not because they are constrained to, but because they are built to care.

Kerstin Dautenhahn. The art of designing socially intelligent agents: Science, fiction, and the human in the loop. *Applied artificial intelligence*, 12(7-8):573–617, 1998.

Alastair Howcroft and Holly Blake. Empathy by design: Reframing the empathy gap between ai and humans in mental health chatbots. *Information*, 16(12):1074, 2025.

Erika Weisz and Mina Cikara. Strategic regulation of empathy. *Trends in Cognitive Sciences*, 25(3):213–227, 2021.

Jean Decety and Philip L. Jackson. The functional architecture of human empathy. *Behavioral*

and *Cognitive Neuroscience Reviews*, 3(2):71–100, 2004.

Claus Lamm, C. Daniel Batson, and Jean Decety. The neural substrate of human empathy: Effects of perspective-taking and cognitive appraisal. *Journal of Cognitive Neuroscience*, 19(1):42–58, 2007.

Simone G. Shamay-Tsoory, Judith Aharon-Peretz, and Daniella Perry. Two systems for empathy: A double dissociation between emotional and cognitive empathy in inferior frontal gyrus versus ventromedial prefrontal lesions. *Brain*, 132(3):617–627, 2009.

Maria Arioli, Zaira Cattaneo, Emiliano Ricciardi, and Nicola Canessa. Overlapping and specific neural correlates for empathizing, affective mentalizing, and cognitive mentalizing: A coordinate-based meta-analytic study. *Human Brain Mapping*, 42(14):4777–4804, 2021.

John M Orbell and Robyn M Dawes. Social welfare, cooperators’ advantage, and the option of not playing the game. *American sociological review*, pages 787–800, 1993.

Matthew Rabin. Incorporating fairness into game theory and economics. *The American economic review*, pages 1281–1302, 1993.

Yu Min Hwang, Issac Sim, Young Ghyu Sun, Heung-Jae Lee, and Jin Young Kim. Game-theory modeling for social welfare maximization in smart grids. *Energies*, 11(9):2315, 2018.

Lindsay M Oberman and Vilayanur S Ramachandran. The simulating social mind: the role of the mirror neuron system and simulation in the social and communicative deficits of autism spectrum disorders. *Psychological bulletin*, 133(2):310, 2007.

Alvin I Goldman. *Simulating minds: The philosophy, psychology, and neuroscience of mindreading*. Oxford University Press, 2006.

Elizabeth Redcay and Leonhard Schilbach. Using second-person neuroscience to elucidate the mechanisms of social interaction. *Nature reviews neuroscience*, 20(8):495–505, 2019.

Konrad Lehmann, Dimitris Bolis, Karl J Friston, Leonhard Schilbach, Maxwell JD Ramstead, and Philipp Kanske. An active-inference approach to second-person neuroscience. *Perspectives on Psychological Science*, 19(6):931–951, 2024.

Daphne Demekas, Conor Heins, and Brennan Klein. An analytical model of active inference in the iterated prisoner’s dilemma. In *International Workshop on Active Inference*, pages 145–172. Springer, 2023.

Riddhi J Pitliya, Ozan Catal, Toon Van de Maele, Corrado Pezzato, and Tim Verbelen. Theory of mind using active inference: A framework for multi-agent cooperation. *arXiv preprint arXiv:2508.00401*, 2025.

- Ozan Çatal, Toon Van de Maele, Riddhi J Pitliya, Mahault Albarracin, Candice Pattisapu, and Tim Verbelen. Belief sharing: a blessing or a curse. In *International Workshop on Active Inference*, pages 121–133. Springer, 2024.
- Tadayuki Matsumura, Kanako Esaki, Shao Yang, Chihiro Yoshimura, and Hiroyuki Mizuno. Active inference with empathy mechanism for socially behaved artificial agents in diverse situations. *Artificial Life*, 30(2):277–297, 2024.
- Ruth M Ford, Timothy Driscoll, David Shum, and Catrin E Macaulay. Executive and theory-of-mind contributions to event-based prospective memory in children: Exploring the self-projection hypothesis. *Journal of experimental child psychology*, 111(3):468–489, 2012.
- Vittorio Gallese and Alvin Goldman. Mirror neurons and the simulation theory of mind-reading. *Trends in cognitive sciences*, 2(12):493–501, 1998.
- Karl Friston, Lancelot Da Costa, Danijar Hafner, Casper Hesp, and Thomas Parr. Sophisticated inference. *Neural Computation*, 33(3):713–763, 2021.
- Lancelot Da Costa, Thomas Parr, Noor Sajid, Sebastijan Veselic, Victorita Neacsu, and Karl Friston. Active inference on discrete state-spaces: A synthesis. *Journal of Mathematical Psychology*, 99:102447, 2020. ISSN 0022-2496. doi:<https://doi.org/10.1016/j.jmp.2020.102447>. URL <https://www.sciencedirect.com/science/article/pii/S0022249620300857>.
- Anatol Rapoport and Albert M. Chammah. *Prisoner’s Dilemma: A Study in Conflict and Cooperation*. University of Michigan Press, 1965.
- David M Kreps. Nash equilibrium. In *The new Palgrave dictionary of economics*, pages 9251–9258. Springer, 2018.
- John F. Nash. Non-cooperative games. *Annals of Mathematics*, 54(2):286–295, 1951.
- Martin J. Osborne and Ariel Rubinstein. *A Course in Game Theory*. MIT Press, 1994.
- Karl J. Friston. Active inference and cognitive consistency. *Psychological Inquiry*, 29(2):67–73, 2018. doi:10.1080/1047840X.2018.1480693.
- Fritz Breithaupt. *The Dark Sides of Empathy*. Cornell University Press, 2019.
- Shannon Spaulding. Motivating empathy. *Mind & Language*, 39(2):220–236, 2024.
- Jamil Zaki. Empathy: A motivated account. *Psychological Bulletin*, 140(6):1608–1647, 2014.
- Joscha Bach. *Principles of Synthetic Intelligence PSI: An Architecture of Motivated Cognition*. Oxford University Press, 2012.